INTERNATIONAL JOURNAL OF QUANTUM CHEMISTRY, VOL. 44, 113–122 (1992)

An Analysis of Molecular Electrostatic Potentials Obtained by a Local Density Functional Approach

JANE S. MURRAY, JORGE M. SEMINARIO, MONICA C. CONCHA, AND PETER POLITZER

Department of Chemistry, University of New Orleans, New Orleans, Louisiana 70148

Abstract

Local density functional theory (DFT–LDA) has been explored as a tool for obtaining the molecular electrostatic potential $V(\mathbf{r})$, using the code DMol. We have presented and discussed DFT–LDA electrostatic potentials for a representative series of molecules: ethylene, benzene, formamide, cytosine, and 2,3,7,8-tetrachlorodibenzo-*p*-dioxin. $V(\mathbf{r})$ results obtained with a double numerical plus polarization (DNP) basis set show the key features that are characteristic of the ab initio potentials of these compounds and suggest that this is a useful approach, especially for large molecules that are difficult to study by ab initio methods.

Introduction

The electrostatic potential $V(\mathbf{r})$ that the nuclei and electrons of a molecule create in the surrounding space is well established as a guide to the interpretation and prediction of molecular reactive behavior [1–7]. It is through this potential $V(\mathbf{r})$, defined rigorously by Eq. (1),

$$V(\mathbf{r}) = \sum_A \frac{Z_A}{|\mathbf{R}_A - \mathbf{r}|} - \int \frac{\rho(\mathbf{r}')d\mathbf{r}'}{|\mathbf{r}' - \mathbf{r}|}, \tag{1}$$

that a molecule is first "seen" or "felt" by an approaching chemical species. Z_A is the charge on nucleus A, located at $\mathbf{R}_A$, and $\rho(\mathbf{r})$ is the electronic density function of the molecule. $V(\mathbf{r})$ has been shown to be a useful tool in studying both electrophilic and nucleophilic processes, including hydrogen-bonding interactions [1–7] and, in particular, to be well suited for studies that involve the identification of key features necessary for the "recognition" of one molecule by another, as in drug-receptor and enzyme–substrate interactions ([3–7], and see, e.g., [8–16]).

An important feature of the electrostatic potential is that it is a real physical property that can be determined experimentally by diffraction methods, as well as computationally [4]. At present, however, computational approaches are the more highly used and practical alternative. In particular, self-consistent-field molecular orbital methods, both ab initio and semiempirical, have been used extensively for obtaining $V(\mathbf{r})$ in the past two decades. Starting with a necessarily approximate $\rho(\mathbf{r})$, $V(\mathbf{r})$ can be evaluated rigorously by Eq. (1) or approximately [3–7]. Various procedures for calculating $V(\mathbf{r})$ have been discussed and analyzed elsewhere [3, 7, 17].

 CCC 0020-7608/92/020113-10$04.00

In addition to the traditional ab initio and semiempirical procedures for computing molecular properties, density functional theory (DFT) techniques are increasingly being used for this purpose [18–22]. This approach is based on the Hohenberg–Kohn theorem, according to which all of the electronic properties of a chemical system, including the energy, can be determined from the electronic density [18]. Density functional theory is commonly applied in the form of the "local density" approximation (LDA), in which the functional relationship between exchange/correlation energy and $\rho(\mathbf{r})$ is expressed in terms of the uniform electron gas model [20, 21]. An important feature of the DFT approach is that it does take account of electron correlation. A key advantage is that the DFT–LDA method requires considerably less computer time and space than do ab initio techniques, thus making it feasible to treat much larger molecules. This is of particular importance in the area of drug design, where interactions between large systems are of primary interest.

It is therefore essential to address the question of the effectiveness of DFT–LDA procedures for computing the molecular electrostatic potential $V(\mathbf{r})$. In this work, we present DFT–LDA potentials for the series of molecules **I–V**; except for **V**, these can be viewed as building blocks of larger systems (e.g., pharmaceuticals, proteins, and nucleic acids). **I–V** have particular electrostatic potential features that help to determine their respective chemical reactivities; these are the negative $V(\mathbf{r})$ associated with (a) heteroatoms containing lone pairs and/or (b) π regions of unsaturated portions of the molecules. Our focus is accordingly on how DFT–LDA procedures reproduce these key features.

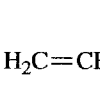

I

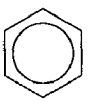

II

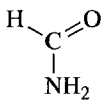

III

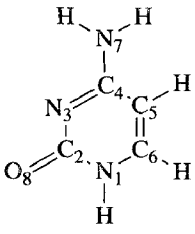

IV

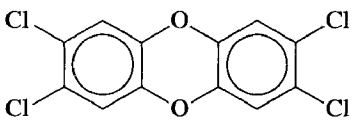

V

Methods and Procedure

We have computed DFT–LDA electrostatic potentials for **I–V** via Eq. (1), using the program DMol [23, 24] with the DN and DNP basis sets. These can be regarded

approximately as double-zeta sets of Slater orbitals, the DNP being augmented by polarization functions. DMol is based on the Kohn–Sham approach [25], in which the electronic density $\rho(\mathbf{r})$ is written as a sum of one-electron orbitals [Eq. (2)],

$$\rho(\mathbf{r}) = \sum_{i=1}^{N} |\varphi_i|^2, \tag{2}$$

which are obtained numerically by solving the Kohn–Sham equations:

$$\left[-\frac{\nabla_i^2}{2} + \nu_{eff}(\mathbf{r}_i)\right]\varphi_i = \varepsilon_i\varphi_i \qquad i = 1,2,\ldots N. \tag{3}$$

As part of the local density approximation, the exchange/correlation contribution to the effective potential, ν_{eff}, is represented by an expression due to von Barth and Hedin [26].

Optimized structures obtained with GAUSSIAN 88 [27] were used for the geometries of **I–IV** (3-21G for **I–III** and STO-3G for **IV**). A crystallographic structure was taken for 2,3,7,8-tetrachlorodibenzo-*p*-dioxin (**V**) [28]; we have also used it in an earlier ab initio SCF–MO study of **V** [29].

Equation (1) shows that $V(\mathbf{r})$ is a sum of a positive contribution coming from the nuclei and a negative one from the electrons; its sign in any particular region depends, therefore, upon whether the effects of the nuclei or the electrons are dominant in that region. An approaching electrophile will initially be attracted to those regions in which $V(\mathbf{r})$ is negative and particularly to the points where $V(\mathbf{r})$ has its most negative values (the local minima, or $V_{\min}$). In the course of very extensive use of the electrostatic potential in interpreting and predicting the reactive behavior of molecules, we have found that negative regions are generally associated with three features [6, 7]: (a) heteroatoms with lone pairs, (b) π regions of unsaturated molecules, and (c) bond regions of strained hydrocarbons. In this work, we investigate the ability of DFT–LDA calculations to reproduce features (a) and (b); these are of particular significance in the behavior of biologically important molecules.

Results and Discussion

Our calculated DFT–LDA/DNP electrostatic potentials of **I–V** are presented in Figures 1–5. These will be discussed in relation to ab initio potentials obtained earlier. Since the magnitudes of these are known to be basis-set dependent [3, 6, 7, 30], we will focus upon qualitative features and relative values.

Figures 1 and 2 show that there are negative potentials above and below the planes of the ethylene and benzene molecules. These are interpreted as being due to the π electrons and indicate these regions to be favorable sites for electrophilic attack [3, 6, 7]. Figures 1 and 2 are qualitatively very similar to ab initio SCF–MO $V(\mathbf{r})$ of **I** and **II**; however, the magnitudes of the $V_{\min}$ at the ab initio SCF–MO STO-5G level are −13 [31] and −11 [32] kcal/mol, respectively, compared to −10 and −18 in Figures 1 and 2.

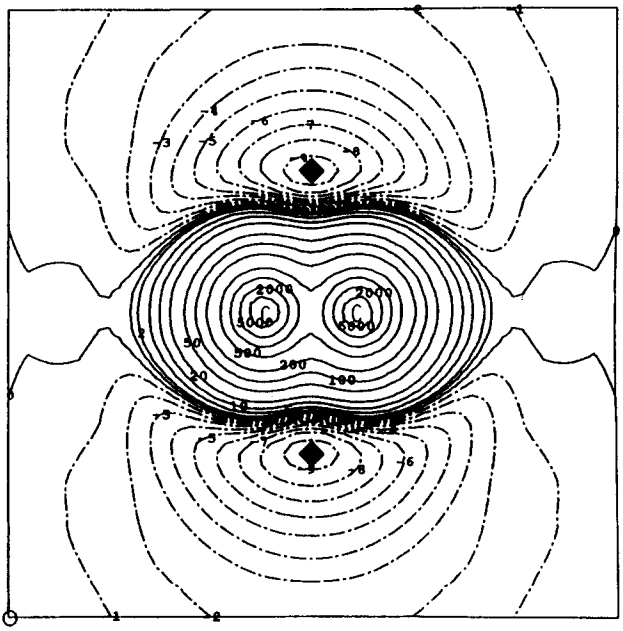

Figure 1. Calculated DFT–LDA/DNP electrostatic potential of ethylene (I), in kcal/mol, in the plane perpendicular to the molecular plane passing through the carbon–carbon double bond. Dashed contours correspond to negative potentials. The positions of the most negative potentials are indicated; the value is (◆) −9.6.

The calculated electrostatic potential of formamide in Figure 3(a) and (b) shows the usual strongly negative region associated with the oxygen. There are no negative potentials by the nitrogen, in contrast to ab initio $V(\mathbf{r})$, which show weak negative regions near it, above and below the molecular plane [1,3,30]. However, these become weaker as one progresses to higher ab initio SCF levels [30], and we find that an MP2/6-311++G** calculation gives nitrogen V_{min} of only −5.4 and −5.1 kcal/mol. The question of the preferred protonation site of formamide has been discussed in detail elsewhere [3]; the general consensus is that oxygen is the primary site for protonation. Both DFT–LDA/DNP and ab initio results support this conclusion.

The DFT–LDA/DNP $V(\mathbf{r})$ of cytosine (**IV**) is shown in Figure 4. There is an extensive negative region associated with N_3 and O_8, with a single V_{min} located in the exocyclic area bordering both N_3 and O_8, suggesting these to be favorable sites for electrophilic attack. Ab initio SCF–MO potentials of **IV**, on the other hand, have separate V_{min} associated with N_3 and O_8, with the V_{min} of N_3 being more negative [3,7,33]. Experimentally, it has been observed that N_3 is the favored site for protonation and alkylation [34–36]. In cases where N_3 is involved in hydrogen bonding, as in DNA, some electrophiles have been observed to react with O_8 [37], while others simply do not react with **IV** at all [36]. Although the DFT–LDA/DNP $V(\mathbf{r})$ of cytosine does not show separate V_{min} for N_3 and O_8, it is generally consistent with the experimental findings; the location of the V_{min} is such as to provide access to either N_3 or O_8.

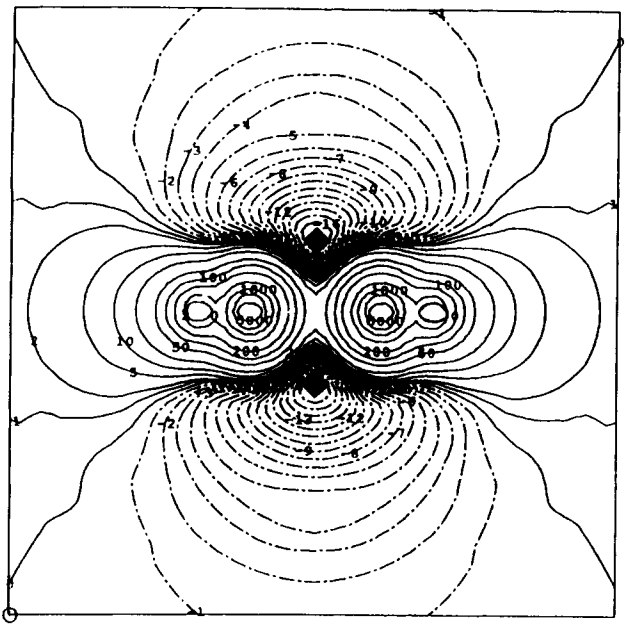

Figure 2. Calculated DFT–LDA/DNP electrostatic potential of benzene (**II**), in kcal/mol, in a plane perpendicular to the molecular plane passing through carbons in the 1- and 4-positions. Dashed contours correspond to negative potentials. The positions of the most negative potentials are indicated; the value is (◆) −17.5.

The $V(\mathbf{r})$ of 2,3,7,8-tetrachlorodibenzo-*p*-dioxin (TCDD, **V**) is of particular interest as an example of the use of the electrostatic potential in recognition interactions [6, 7, 29]. TCDD is generally viewed as a highly toxic compound, while the nonchlorinated parent molecule, dibenzo-*p*-dioxin, is biologically inactive [38]. The toxic responses associated with TCDD and other active dibenzo-*p*-dioxins are believed to be initiated through a recognition interaction with a cytosolic receptor. In earlier ab initio SCF–MO studies [6, 29, 39–41], we have identified key $V(\mathbf{r})$ features and patterns that appear to be necessary for high activity in these systems. These are (a) negative regions above all or most of the lateral portions of the molecule (e.g., outside positions 2,3 and 7,8 in the dibenzo-*p*-dioxin framework) and (b) primarily positive potential above the central part of the molecule. (It appears necessary that the characteristic negative regions normally associated with oxygens be small and weak in the active dibenzo-*p*-dioxins [6, 29, 39–41].)

It can be seen in Figure 5 that the DFT–LDA/DNP $V(\mathbf{r})$ of **V** qualitatively fulfills the requirements for high activity outlined above. However, there are a few qualitative and quantitative differences between our earlier ab initio SCF–MO potentials of TCDD and that obtained in the present work. In Figure 5, for example, very weak oxygen potentials can be seen at 1.75 Å above the plane of the molecule. These were not observed in the ab initio results at this distance [6, 29]. Second, there is now a third minimum above the central area of each lateral region, associated with the chlorines; only two were observed earlier. Despite

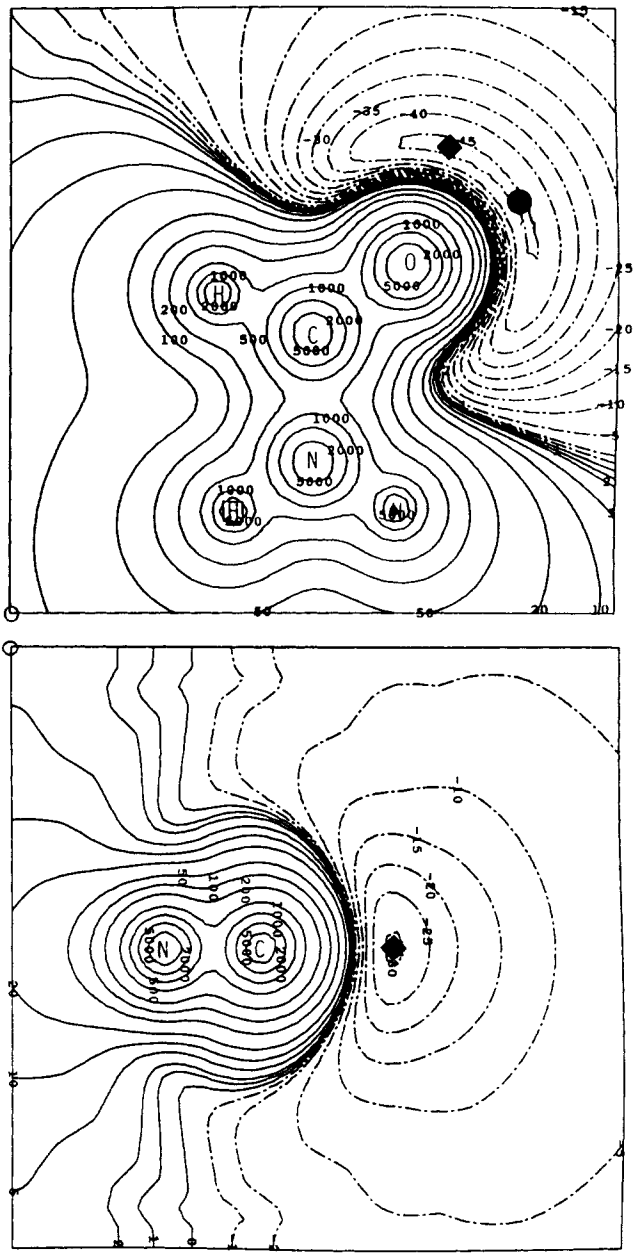

Figure 3. Calculated DFT–LDA/DNP electrostatic potential of formamide (**III**), in kcal/mol, in (a) the plane defined by C, N, and O, and (b) the plane perpendicular to the C, N, O plane passing through the C—N bond. Dashed contours correspond to negative potentials. The positions of the most negative potentials are indicated; the values are (a) (◆) −46.0, (●) −45.4; (b) (◆) −30.6.

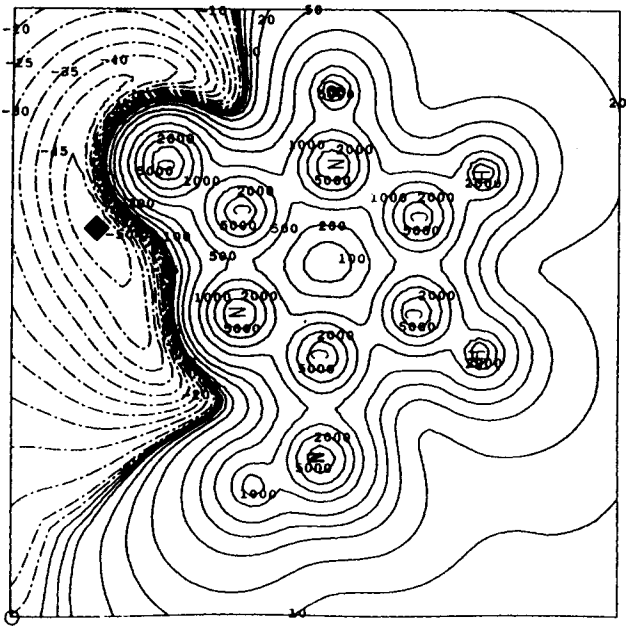

Figure 4. Calculated DFT–LDA/DNP electrostatic potential of cytosine (**IV**), in kcal/mol, in the plane of the six-membered ring. Dashed contours correspond to negative potentials. The position of the most negative potential is indicated; the value is (◆) −55.3.

these differences, the DFT–LDA/DNP $V(\mathbf{r})$ of TCDD does show, overall, the key features and pattern that we have earlier related to high activity in the dibenzo-*p*-dioxins.

The $V(\mathbf{r})$ shown in Figures 1–5 were computed using the DNP basis set. We have also calculated the electrostatic potentials of **I**–**V** at the DFT–LDA/DN level (i.e., without polarization functions). For **I**–**III**, these show qualitatively the same features as the DFT–LDA/DNP results: negative regions attributed to the π electrons in **I** and **II** and a large, strongly negative one associated with the oxygen in **III**.

However, the DFT–LDA/DN potentials of cytosine and TCDD differ significantly from both the ab initio and the DFT–LDA/DNP. At the DFT–LDA/DN level, there are two V_{min} in the ring plane of **IV**, associated with N_3 and O_8; however, the latter is the more negative, which is inconsistent with the experimental observations mentioned earlier. In Figure 6, we present a DFT–LDA/DN electrostatic potential of TCDD. The $V(\mathbf{r})$ features that we have earlier identified as being necessary for high biological activity in the dibenzo-*p*-dioxins are not at all well reproduced in Figure 6. The oxygen negative regions are now quite strong, and there are negative potentials above the aromatic rings as well as above the lateral portions of the molecule. While π regions of aromatics do in many instances show characteristic negative potentials (e.g., see Fig. 2), our experience has shown that these are essentially eliminated by substitution of strongly electron-

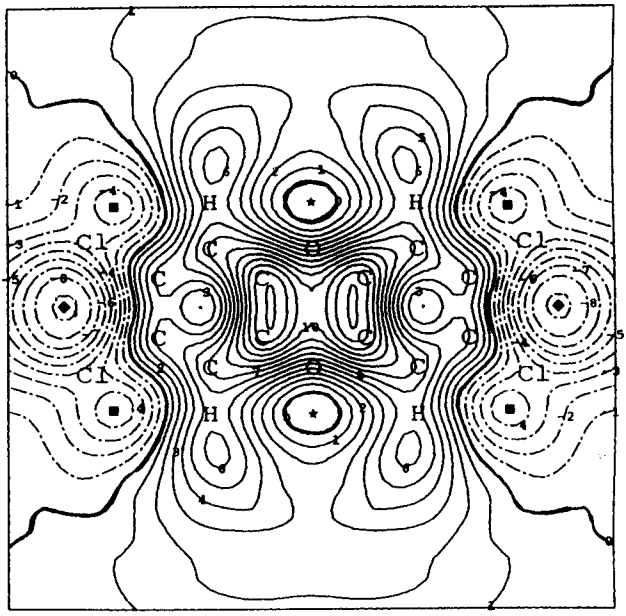

Figure 5. Calculated DFT–LDA/DNP electrostatic potential of 2,3,7,8-tetrachlorodibenzo-*p*-dioxin (V), in kcal/mol, in the plane 1.75 Å above the molecular plane. The projections of the nuclear positions are shown by their atomic symbols. Dashed contours correspond to negative potentials. The positions of the most negative potentials are indicated; the values are (◆) −9.4; (■) −4.7; (★) −1.1.

withdrawing groups or atoms, such as Cl or NO_2 [3, 6, 7, 29, 32, 39–41]. It can be concluded, therefore, that the DN basis set does not consistently produce molecular electrostatic potentials that are even qualitatively reliable.

Summary

We have presented and discussed DFT–LDA/DNP electrostatic potentials for a representative group of molecules: ethylene, benzene, formamide, cytosine, and 2,3,7,8-tetrachlorodibenzo-*p*-dioxin. Our results do, in general, show the key $V(\mathbf{r})$ features that characterize the ab initio potentials of these compounds, although there are significant differences in detail. It may be that these would be diminished by the use of a basis set larger than DNP. We do feel that the DFT–LDA/DNP approach is a promising one, especially for large molecules that are difficult to study by ab initio methods. On the other hand, the use of the DN basis set is not recommended for this purpose.

Acknowledgment

We greatly appreciate the support of the Office of Naval Research through contract number N00014-85-K-0217.

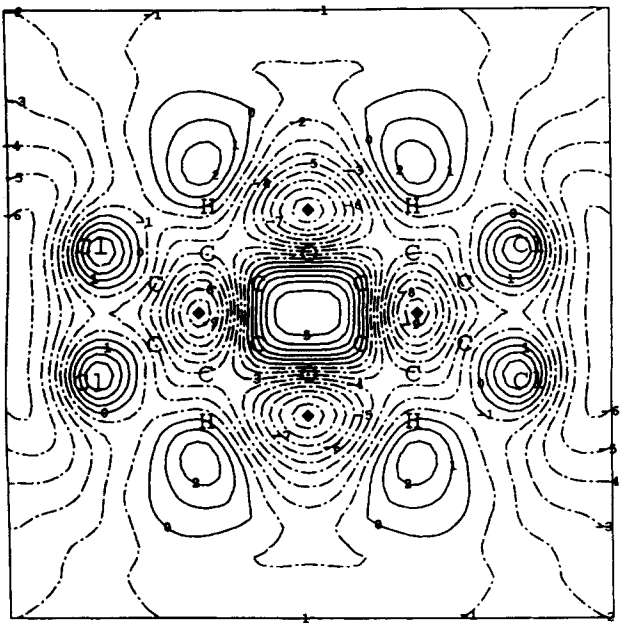

Figure 6. Calculated DFT–LDA/DN electrostatic potential of 2,3,7,8-tetrachlorodibenzo-*p*-dioxin (**V**), in kcal/mol, in the plane 1.75 Å above the molecular plane. The projections of the nuclear positions are shown by their atomic symbols. Dashed contours correspond to negative potentials. The positions of the most negative potentials are indicated; the value is (◆) −9.6.

Bibliography

[1] E. Scrocco and J. Tomasi, in *Topics in Current Chemistry,* No. 42 (Springer-Verlag, Berlin, 1973), p. 95.

[2] E. Scrocco and J. Tomasi, Adv. Quantum Chem. **11**, 115 (1978).

[3] P. Politzer and K. C. Daiker, in *The Force Concept in Chemistry,* B. M. Deb, Ed. (Van Nostrand Reinhold, New York, 1981), Chap 6.

[4] P. Politzer and D. G. Truhlar, Eds., *Chemical Applications of Atomic and Molecular Electrostatic Potentials* (Plenum, New York, 1981).

[5] P. Politzer, P. R. Laurence, and K. Jayasuriya, in *Structure-Activity Correlation in Mechanism Studies and Predictive Toxicology,* J. McKinney, Ed., Environ. Health Perspectives (Special Issue) **61**, 191 (1985).

[6] P. Politzer and J. S. Murray, in *Theoretical Biochemistry and Molecular Biophysics: A Comprehensive Survey,* D. L. Beveridge and R. L. Lavery, Eds. (Adenine Press, Schenectady, NY, 1990).

[7] P. Politzer and J. S. Murray, in *Reviews of Computational Chemistry,* K. B. Lipkowitz and D. B. Boyd, Eds. (VCH, New York, 1991), Chap. 7.

[8] Z. Paster, S. Maayani, H. Weinstein, and M. Sokolovsky, Eur. J. Pharmacol. **25**, 270 (1974).

[9] C. Petrongolo and J. Tomasi, Int. J. Quantum Chem., Quantum Biol. Symp. **2**, 181 (1975).

[10] G. H. Loew and D. S. Berkowitz, J. Med. Chem. **18**, 656 (1975).

[11] D. M. Hayes and P. A. Kollman, J. Am. Chem. Soc. **98**, 7811 (1976).

[12] H. Weinstein, R. Osman, S. Topiol, and J. P. Green, Ann. N.Y. Acad. Sci. **367**, 434 (1981).

[13] B.V. Cheney, D. A. Zichi, and A. B. Miller, Int. J. Quantum Chem., Quantum Biol. Symp. **10**, 43 (1983).

[14] A. P. Mazurek, H. Weinstein, R. Osman, S. Topiol, and B. J. Ebersole, Int. J. Quantum Chem., Quantum Biol. Symp. **11**, 183 (1984).
[15] S. Guha and D. Majumdar, Int. J. Quantum Chem., Quantum Biol. Symp. **13**, 19 (1986).
[16] R. Bonaccorsi, M. Hodoscek, and J. Tomasi, J. Mol. Struct. (Theochem) **164**, 105 (1988).
[17] J. Tomasi, in *Molecular Interactions,* H. Ratajczak and W. J. Orville-Thomas, Eds. (Wiley, New York, 1982), Vol. 3, pp. 119–181.
[18] P. Hohenberg and W. Kohn, Phys. Rev. B **136**, 864 (1964).
[19] J. P. Dahl and J. Avery, Eds., *Local Density Approximations in Quantum Chemistry and Solid State Physics* (Plenum Press, New York, 1984).
[20] R. G. Parr and W. Yang, *Density Functional Theory of Atoms and Molecules* (Oxford University Press, New York, 1989).
[21] E. S. Kryachko and E.V. Ludena, *Energy Density Functional Theory of Many-Electron Systems* (Kluwer, Dordrecht, The Netherlands, 1990).
[22] J. K. Labanowski and J.W. Andzelm, Eds., *Density Functional Methods in Chemistry* (Springer, New York, 1991).
[23] B. Delley, J. Chem. Phys. **92**, 508 (1990).
[24] DMol, from Biosym Technologies, Inc.
[25] W. Kohn and L. J. Sham, Phys. Rev. B **31**, 7588 (1985).
[26] U. von Barth and L. Hedin, J. Phys. C **5**, 1629 (1972).
[27] M. J. Frisch, M. Head-Gordon, H. B. Schlegel, K. Raghavachari, J. S. Binkley, C. Gonzalez, D. J. Defrees, D. J. Fox, R. A. Whiteside, R. Seeger, C. F. Melius, J. Baker, R. Martin, L. R. Kahn, J. J. P. Stewart, E. M. Fluder, S. Topiol and J. A. Pople, GAUSSIAN 88 (Gaussian Inc., Pittsburgh, PA, 1988).
[28] F. B. Boer, F. P. Van Remoortere, P. P. North, and M. A. Newman, Acta Cryst. Sect. B: Struct. Crystallogr. Cryst. Chem. B **28**, 1023 (1972).
[29] J. S. Murray, B. A. Zilles, K. Jayasuriya, and P. Politzer, J. Am. Chem. Soc. **108**, 915 (1986).
[30] J. M. Seminario, J. S. Murray, and P. Politzer, in *The Application of Charge Density Research to Chemistry and Drug Design,* G. A. Jeffrey and J. F. Piniella, Eds. (Plenum Press, New York, 1991), p. 371.
[31] P. Politzer and W. L. Hedges, Int. J. Quantum Chem.; Quantum Biol. Symp. **9**, 307 (1982).
[32] P. Politzer, L. Abrahmsen, and P. Sjoberg, J. Am. Chem. Soc. **106**, 855 (1984).
[33] R. Bonaccorsi, A. Pullman, E. Scrocco, and J. Tomasi, Theor. Chim. Acta **24**, 51 (1972).
[34] P. Brookes and P. D. Lawley, J. Chem. Soc. 1348 (1962).
[35] O. Jardetzky, P. Pappas, and N. G. Wade, J. Am. Chem. Soc. **85**, 1675 (1963).
[36] P. D. Lawley, Prog. Nucl. Acid Res. Mol. Biol. **5**, 89 (1966).
[37] N. F. Dove, F. A. Wallace, and N. Davidson, Biochem. Biophys. Res. Commun. **1**, 319 (1959).
[38] A. Poland and J. C. Knutson, Annu. Rev. Pharmacol. Toxicol. **22**, 517 (1982).
[39] J. S. Murray and P. Politzer, Theor. Chim. Acta **72**, 507 (1987).
[40] J. S. Murray, P. Evans, and P. Politzer, Int. J. Quantum Chem. **37**, 271 (1990).
[41] P. Sjoberg, J. S. Murray, T. Brinck, P. Evans, and P. Politzer, J. Mol. Graph. **8**, 81 (1990).

Received September 10, 1991
Revised manuscript received October 7, 1991
Accepted for publication October 14, 1991